

Ser
TH1
N21d
no. 1567
c. 2
BLDG

**National Research
Council Canada**

**Conseil national
de recherches Canada**

**Institute for
Research in
Construction**

**Institut de
recherche en
construction**

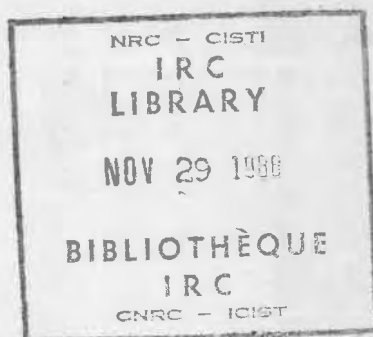
Experimental Procedures for Determination of Dynamic Response Using System Identification Techniques

by F. Haghighat and D.M. Sander

ANALYZED

Reprinted from
Journal of Thermal Insulation
Vol. 11 — October 1987
p. 120-143
(IRC Paper No. 1567)

NRCC 29651



Canada

8469758

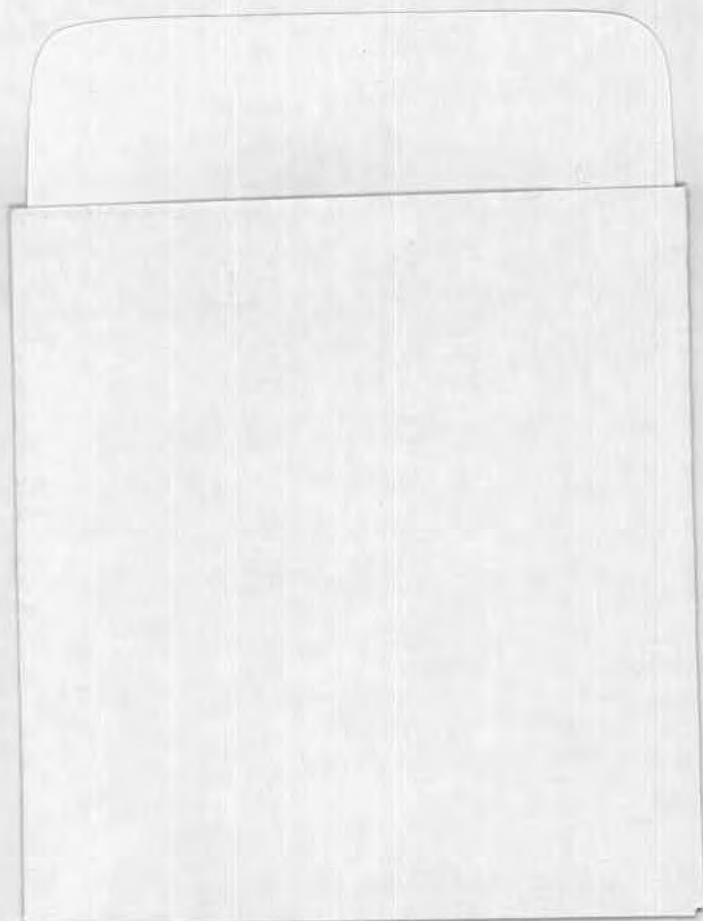
CISTI / ICIST



3 1809 00210 7495

RÉSUMÉ

Les auteurs examinent des méthodes servant à déterminer la réponse thermique dynamique à l'aide de techniques d'identification de systèmes. Ils décrivent un essai utilisant en entrée une séquence multifréquence binaire pour déterminer la réponse d'un échantillon de matériau. Ils obtiennent les coefficients de fonction de transfert z au moyen du calcul de la réponse de fréquence et de la régression par la méthode des moindres carrés en domaine de temps.



Experimental Procedures for Determination of Dynamic Response Using System Identification Techniques

F. HAGHIGHAT

*Center for Building Studies
Concordia University
Montreal, Quebec
H3G 1M8 Canada*

D. M. SANDER

*National Research Council Canada
Institute for Research in Construction
Ottawa, Ontario, Canada K1A 0R6*

ABSTRACT

Methods for determining dynamic thermal response using systems identification techniques are discussed. A test using a binary multi-frequency sequence as input to determine the response of a material sample is described. Z-transfer function coefficients are obtained using both frequency response analysis and least squares regression in time domain.

INTRODUCTION

KNOWLEDGE OF THE dynamic response of building envelope components is important in the design of thermal systems. The load calculation method given in the ASHRAE Handbook [1] is based on the "z-transfer function" method developed by Stephenson and Mitalas [2]. The coefficients for walls and roofs are obtained either from tables contained in the Handbook or by means of a computer program [3]. In either case, these coefficients are derived from an analytical method which assumes that the construction consists of layers of homogenous material and that heat flow is

Reprinted from *JOURNAL OF THERMAL INSULATION* Volume 11—October 1987

one-dimensional. In practice, actual walls contain heat bridges, such as studs or structural members, and may be composed of non-homogenous materials. Furthermore, the properties of the materials may be unknown or difficult to determine. Therefore, there is a need for experimental methods to determine the dynamic thermal performance of components.

This paper discusses some of the procedures for determining dynamic response, and describes a test on a slab of homogeneous material to demonstrate one of these techniques.

A complete dynamic model for heat flow through a component is commonly represented in the matrix notation introduced by Pipes [4] which relates the temperatures and heat flows at both surfaces (see Figure 1).

$$\begin{bmatrix} \Theta_1 \\ Q_1 \end{bmatrix} = \begin{bmatrix} A & B \\ C & D \end{bmatrix} \cdot \begin{bmatrix} \Theta_2 \\ Q_2 \end{bmatrix} \quad (1)$$

The transfer function of interest for load calculations is $-1/B$, which relates the heat flow at the inside surface, Q_2 , to the temperature at the outside surface, Θ_1 , with the boundary condition of a constant inside temperature, Θ_2 .

$$H = \frac{Q_2}{\Theta_1} \quad \left| \quad \Theta_2 = \text{constant} \right. \quad (2)$$

In z -transfer function form this is written as

$$H(z) = \frac{a_0 + a_1 Z^{-1} + a_2 Z^{-2} + \dots a_n Z^{-n}}{1 + b_1 Z^{-1} + b_2 Z^{-2} + \dots b_m Z^{-m}} \quad (3)$$

This transfer function is used to simulate the response by calculating heat

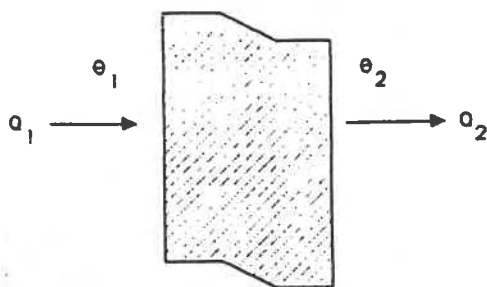


FIGURE 1. Heat flow through a component.

flux Q_2 at time t from a history of values for Q_2 and Θ_1 ,

$$Q_{2(t)} = \sum_{i=0}^n a_i \Theta_1(t - i\Delta) - \sum_{i=1}^m b_i Q_2(t - i\Delta) \quad (4)$$

where Δ is the time interval for the simulation.

SYSTEM IDENTIFICATION

The use of system identification methods to determine parameters of a system is well established [5,6]. These are methods of obtaining a mathematical model for a system on the basis of analysis of input and output signals. This requires both selection of the form of the model (i.e., the equation) and estimation of values for the parameters in the model. The existence of many different solutions for a given system is common. There is generally a compromise between modelling error and complexity. Therefore, the selection of the model depends upon the purpose of the identification and the experience of the user. While system identification techniques may employ non-linear models, the techniques described in this paper are applicable only when linearity can be assumed. Both the z -transfer function and the Fourier transform are valid only for linear systems. Heat transfer problems are normally considered linear, but this may be inappropriate in some cases such as when heat transfer is primarily by radiation or when moisture is present in a porous material.

Various input signals may be employed. A step input is the simplest for the purpose of system identification. This signal provides a good insight into the transient response of the system. For a first-order system the steady state gain and time constant may easily be determined. Methods also exist [7] to identify higher order systems. Similarly, the parameters of a system can be obtained using a ramp input signal [8], since a ramp is the integral of a step function. For a linear system, the relationship between the input, $x(t)$, and the output, $y(t)$, is given by the convolution integral

$$y(t) = \int h(u)x(t - u)du \quad (5)$$

where $h(u)$, the weighting function, describes the dynamic characteristics of the system. Therefore, theoretically, a unit impulse would be the ideal input signal since the resulting output would be the weighting function $h(u)$. (The weighting function is essentially the same as the response factors referred to by Mitalas [9].) However, in practice it is impossible to produce a true im-

pulse and difficult to achieve an approximation which has sufficient magnitude to yield a usable output.

Frequency response analysis is a classical technique in control engineering and may be used for identification of systems. In its basic form, a sinusoidal input is applied to the system. The system response, at this frequency, can be described by the ratio of amplitude of output to input and the difference in phase between output and input. Repeating for several frequencies provides enough information to plot the amplitude ratio and phase lag versus frequency to indicate the system frequency response. The disadvantages of this procedure are that it may be difficult to produce a sinusoidal signal and a series of tests takes a long time.

These disadvantages may be overcome by Fourier analysis techniques. A periodic signal containing many frequency components is applied to the input. A Fourier transform is then performed on both input and output; the result is sufficient information to produce a Bode plot from a single test.

Equation (5) can be transformed to frequency domain as

$$Y(\omega) = H(\omega)X(\omega) \quad (6)$$

where

$Y(\omega)$ — Fourier transform of output, $y(t)$

$X(\omega)$ — Fourier transform of input, $x(t)$

$H(\omega)$ — transfer function, Fourier transform of $h(u)$

Therefore, $H(\omega)$ can be obtained from Equation (6), and an inverse Fourier transform of $H(\omega)$ will yield the describing function $h(u)$.

A convenient type of input signal for Fourier analysis is a binary periodic sequence [10]. This signal is easy to generate by simply switching between two states (on/off); it does not require any complex control or waveform generator. Pseudo-random binary signals are often used when frequency response at many points over a wide frequency range is required. Other forms of binary multi-frequency signal (BMFS) have the characteristic that their power is concentrated in a limited number of frequencies. While this signal gives response information for fewer points over a smaller frequency bandwidth, it has the advantage that the amplitude of those frequency components is larger and less susceptible to noise. This type of signal is well suited to response evaluation of systems that have non-resonance or non-rejection response characteristics and was, for this reason, used in the experimental procedure to be described in the following section.

Least squares techniques have also been employed to fit parameter values to a chosen transfer function model in time domain [11]. These attempts

have encountered difficulty in fitting directly to the z -transfer coefficients of Equation (4). Pedersen and Mouen [12] found the direct solution produced meaningless response factors and chose instead to estimate values of equivalent thermophysical properties (conductivity, density and specific heat) using a stochastic gradient algorithm. Sherman et al. [13] defined a set of simplified thermal parameters and used them to characterize the thermal performance of the wall from an arbitrary temperature history using digital filter design.

DESCRIPTION OF TEST APPARATUS AND PROCEDURE

An experiment was performed at the Thermal Insulation Laboratory of the Institute for Research in Construction, National Research Council Canada, to investigate test procedures for determining the dynamic heat transfer characteristics of a slab of material. The sample chosen was a sheet of rubber material for which the thermal properties (see Appendix A) were known.

The requirements for determination of H are to:

- introduce a variation in Θ_1 , the temperature on surface 1
- measure Q_2 , the heat flux at surface 2
- maintain constant Θ_2 , the temperature of surface 2

The simple heat flow meter configuration shown in Figure 2, using a heat flux transducer to measure Q_2 , is not satisfactory. The problem is that a temperature drop, proportional to Q_2 , appears across the heat flux transducer.

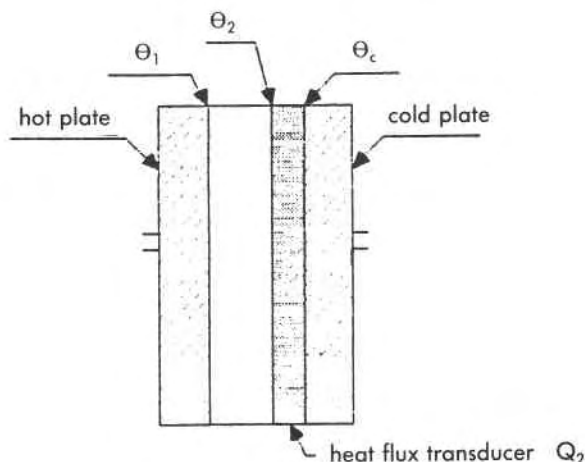


FIGURE 2. Heat flow meter apparatus.

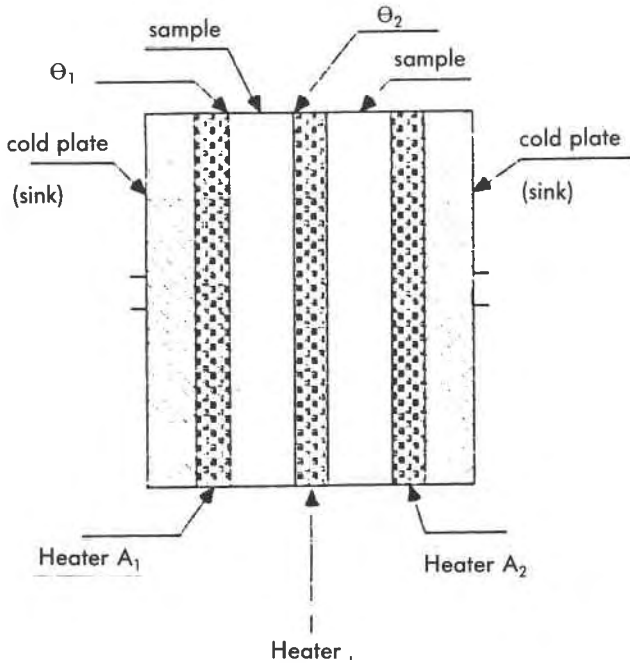


FIGURE 3. Schematic of test apparatus.

Therefore, temperature Θ_2 varies, even though the cold plate temperature Θ_c is kept constant. (An additional difficulty is that the frequency response of the heat flux transducer must be broad enough to cover the frequencies of the test.)

A modification of the 600 mm heat flow apparatus [14], shown in Figure 3, was used. Temperature Θ_2 is maintained constant by an electric heater and temperature controller. This heater consists of a metering area surrounded by a guard area, as shown in Figure 4. The guard area is maintained at the same temperature as the metered area to prevent edge losses. The power input, P , to the metering area is measured. Because of symmetry, if the temperature Θ_2 is maintained perfectly constant the heat flux at the surface is

$$Q_2 = \frac{P}{2A} \quad (7)$$

where A is the metered area.

Temperature Θ_1 was varied by switching heaters A_1 and A_2 on and off. The cold plates were kept at a constant temperature to serve as a sink for the heat

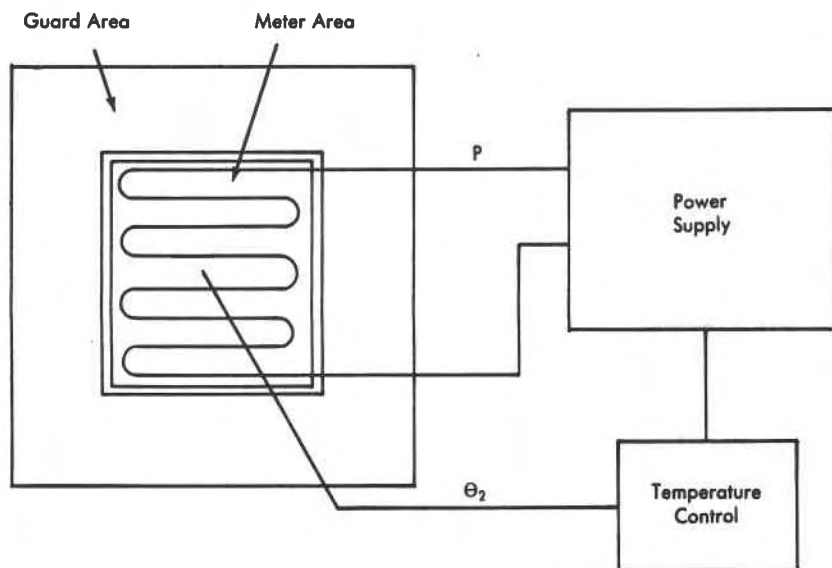


FIGURE 4. Schematic of measurement apparatus.

from the heaters. A computer data acquisition system recorded data every 15 seconds.

RESULTS

A binary multi-frequency sequence, shown in Figure 5(a), was used as the signal to control the heaters A_1 and A_2 . This signal was obtained from the following equation, where the heaters are on when $g(t) \geq 0$ and off when $g(t) \leq 0$.

$$g(t) = \cos(\omega) - \cos(2\omega) + \cos(4\omega) - \cos(8\omega) + \cos(16\omega) - \cos(32\omega) + \cos(64\omega) \quad (8)$$

where

$$\omega = \frac{2\pi t}{T}$$

and T = period of the sequence. Figure 5(b) shows the amplitude of the frequency spectrum of this signal.

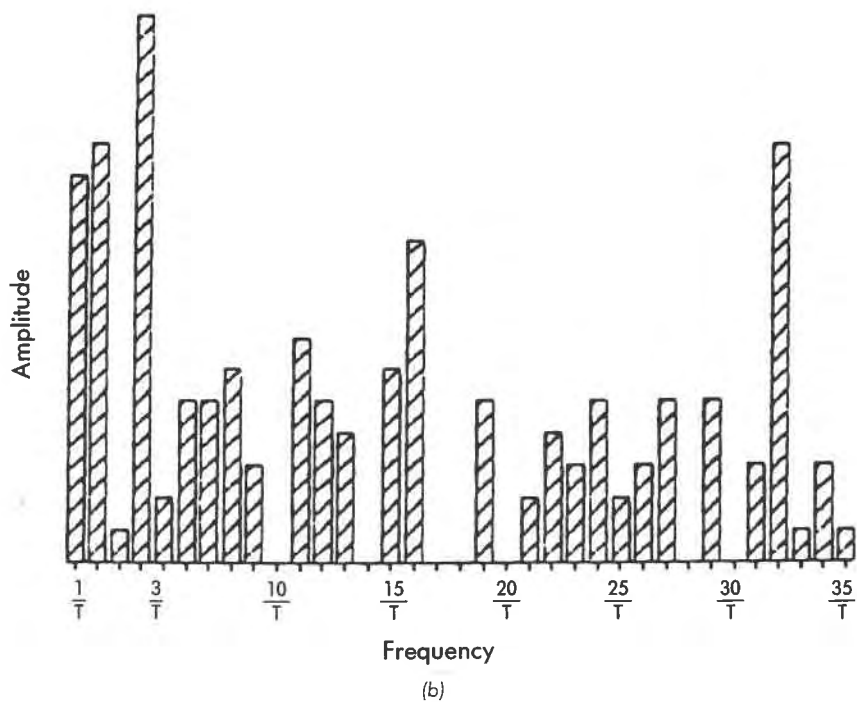
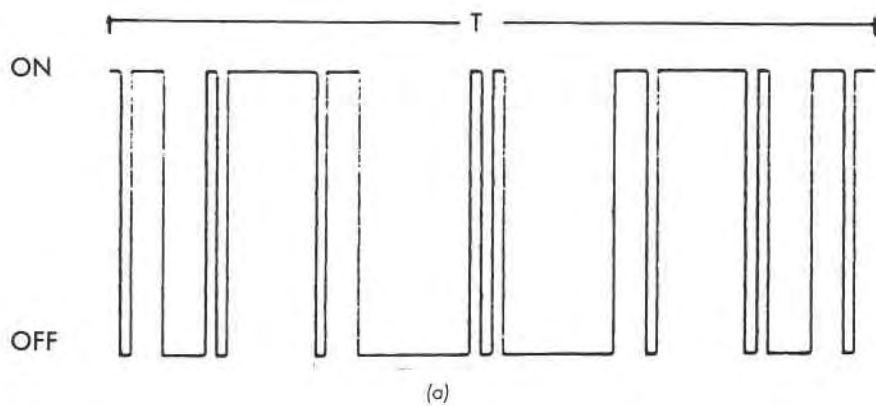


FIGURE 5. (a) A multifrequency binary sequence signal with period T ; (b) amplitude of frequency components of the signal.

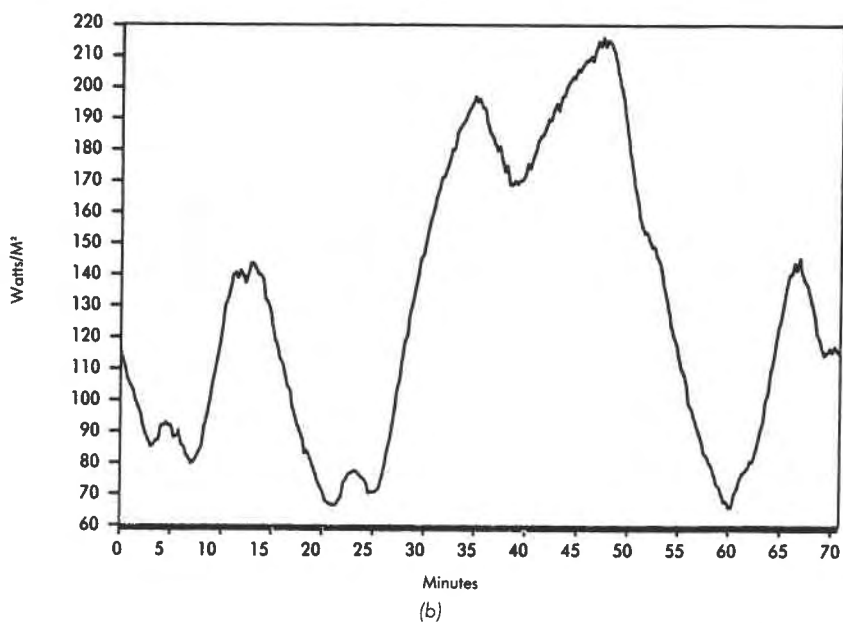
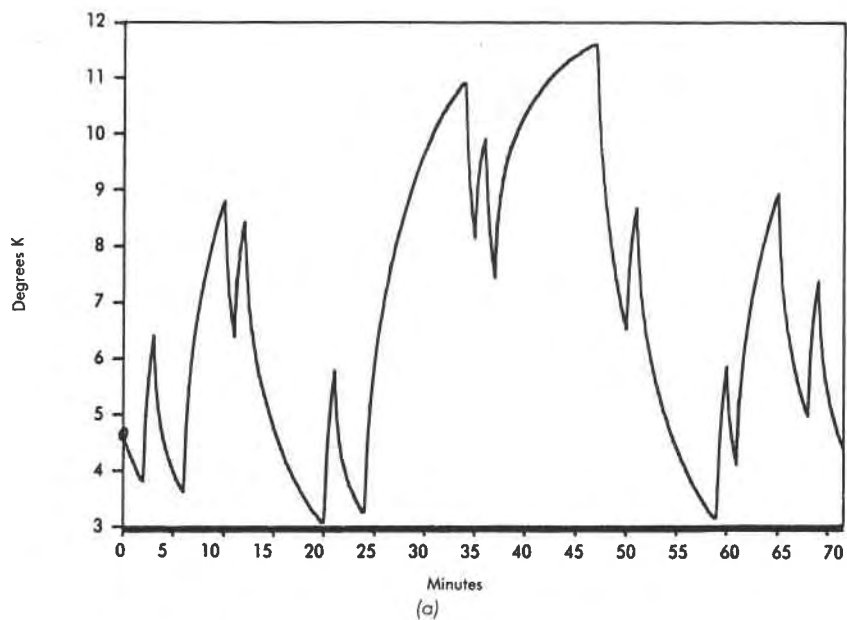


FIGURE 6. (a) Temperature, θ_1 (test input); (b) heat flux, Q_2 (test output).

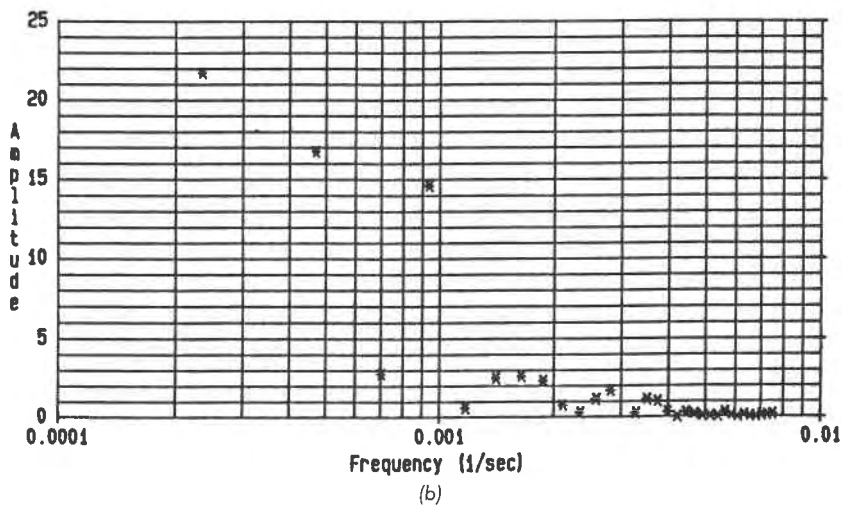
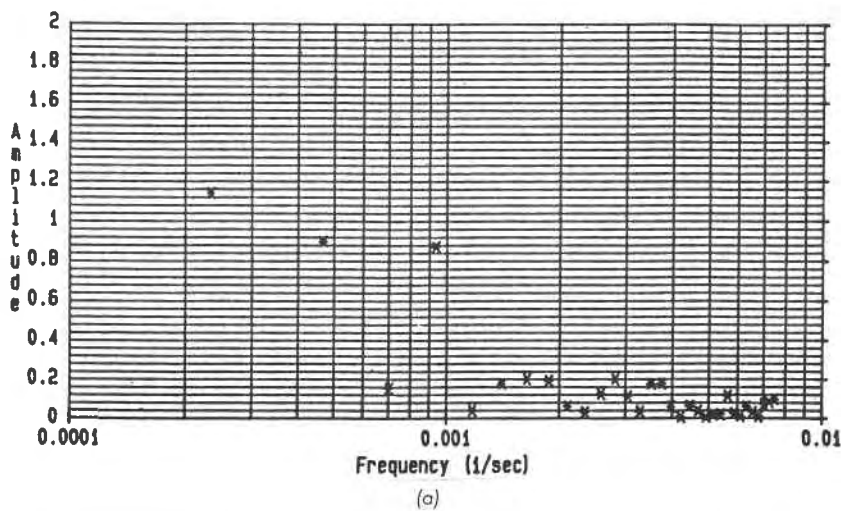


FIGURE 7. (a) Amplitude of frequencies in the input signal, θ_1 (degrees C); (b) amplitude of frequencies in the output signal, Q_2 (w/m²).

The resulting temperature Θ_1 and heat flow Q_2 , after a periodic condition had been established (after 6 periods), are shown in Figure 6. Figure 7 shows the results of Fourier analysis using a fast Fourier transform [15,16].

The transfer function $H(\omega)$ was obtained from Equation (6). To reduce the effect of noise, only frequencies at which $\Theta_1(\omega)$ had a reasonably large amplitude (greater than 0.1) were considered; 14 frequencies met this criterion.

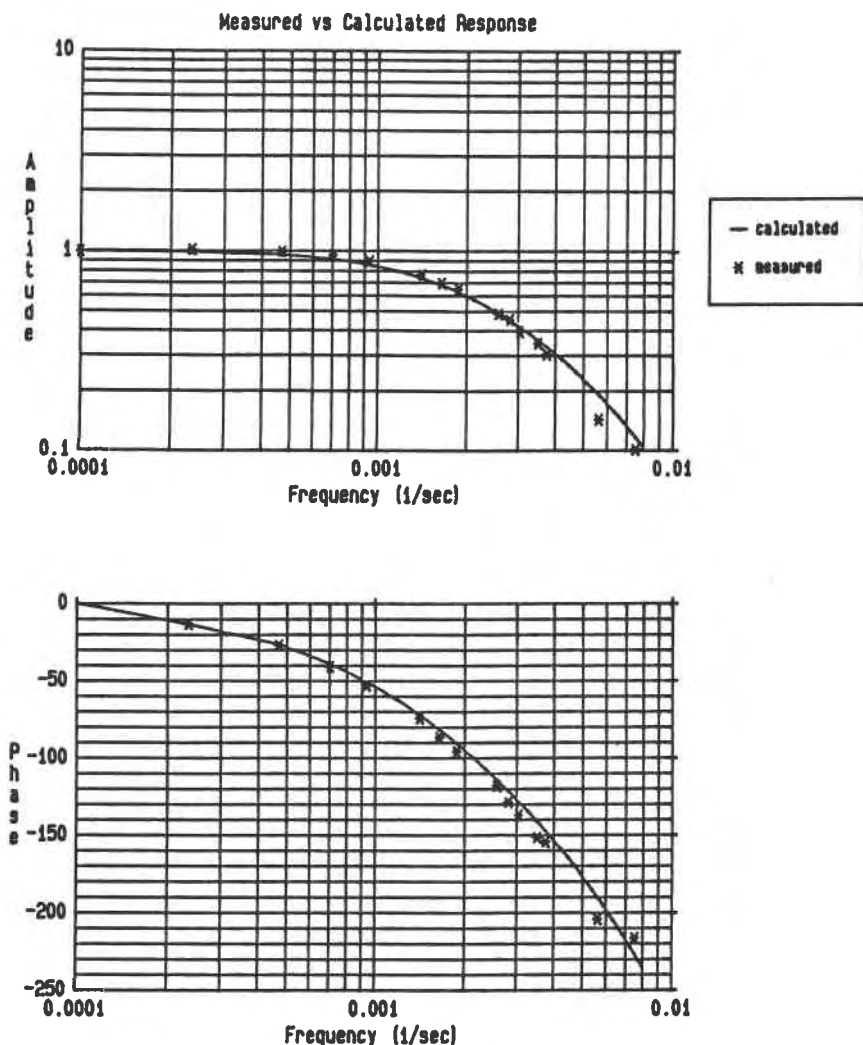


FIGURE 8. Frequency response obtained from test measurements; theoretical calculated response shown for comparison.

The resulting transfer function, normalized to U -value, is shown in Figure 8. For comparison, the theoretically derived frequency response for the slab of rubber material is also shown.

The agreement between the theoretical and experimental response is good. However, the experimental values show a slight resonance characteristic which would not be associated with the heat transfer process; the amplitude ratio at the first harmonic is slightly greater than at steady state. Further investigation revealed that the temperature controller was not maintaining temperature Θ_2 constant. The frequencies of this variation in Θ_2 were those displaying the resonance phenomena. The apparent resonance is therefore attributed to error introduced by variation of the temperature of mass of the heater. This highlights the importance of good control when using this approach to measuring heat flow.

Although the frequency response function $H(\omega)$ is very useful, the z -transfer function form is required for load calculations or time-domain thermal simulation. A regression technique can be applied directly to the measured frequency response data, to fit coefficients to a transfer function of the form given in Equation (4). In addition to one equation for steady state, two equations can be written for each frequency: one for the real component and one for the imaginary component (see Appendix B).

Therefore, for 14 measured frequencies, 29 equations can be written and regression used to solve for the coefficients. Table 1 gives the coefficients obtained for different numbers of terms in the numerator and denominator. Higher orders than those shown in Table 1 resulted in unstable simulations. Figure 9 shows the frequency response plots for these derived z -transfer functions. Table 3 gives the response of the z -transfer functions compared to the measured response.

Table 1. Z -transfer function coefficients from frequency analysis ($\Delta = 60$ sec).

| n | m | a_0 | a_1 | a_2 | a_3 | a_4 | b_1 | b_2 | b_3 | b_4 |
|---|---|-------|-------|-------|-------|-------|-------|-------|-------|-------|
| 2 | 1 | 0.0 | 0.223 | 0.212 | | | -.565 | | | |
| 3 | 1 | 0.0 | 0.229 | 0.219 | 0.038 | | -.515 | | | |
| 4 | 1 | 0.0 | 0.230 | 0.223 | 0.044 | 0.007 | -.497 | | | |
| 2 | 2 | 0.0 | 0.233 | 0.175 | | | -.700 | 0.107 | | |
| 3 | 2 | 0.0 | 0.233 | 0.178 | 0.003 | | -.625 | -.098 | | |
| 4 | 2 | 0.0 | 0.233 | 0.192 | 0.016 | 0.005 | -.626 | 0.072 | | |
| 2 | 3 | 0.0 | 0.233 | 0.208 | | | -.579 | -.043 | 0.062 | |
| 3 | 3 | 0.0 | 0.228 | 0.272 | 0.056 | | -.308 | -.210 | 0.074 | |
| 4 | 3 | 0.0 | 0.220 | 0.306 | -.040 | -.112 | -.227 | -.748 | 0.348 | |
| 2 | 4 | 0.0 | 0.230 | 0.228 | | | -.494 | -.168 | 0.162 | -.044 |
| 3 | 4 | 0.0 | 0.230 | 0.227 | -.001 | | -.498 | -.165 | 0.163 | -.044 |

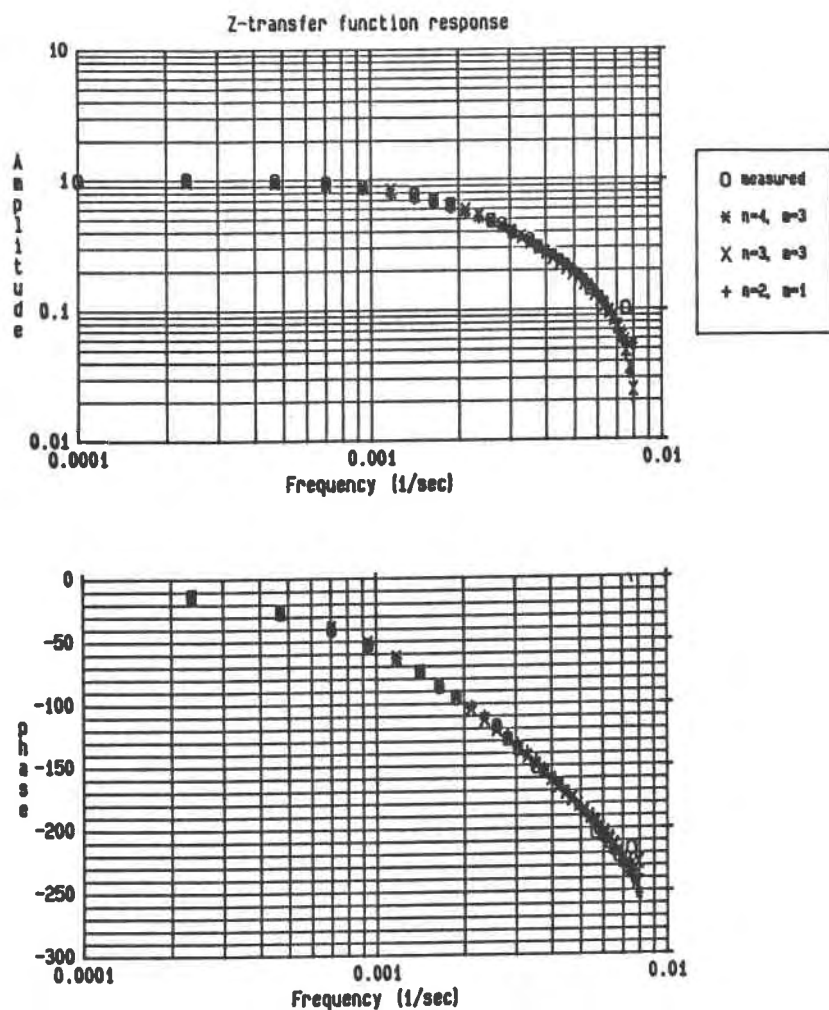


FIGURE 9. Frequency response of z -transfer functions. Coefficients, obtained from test, are given in Table 1.

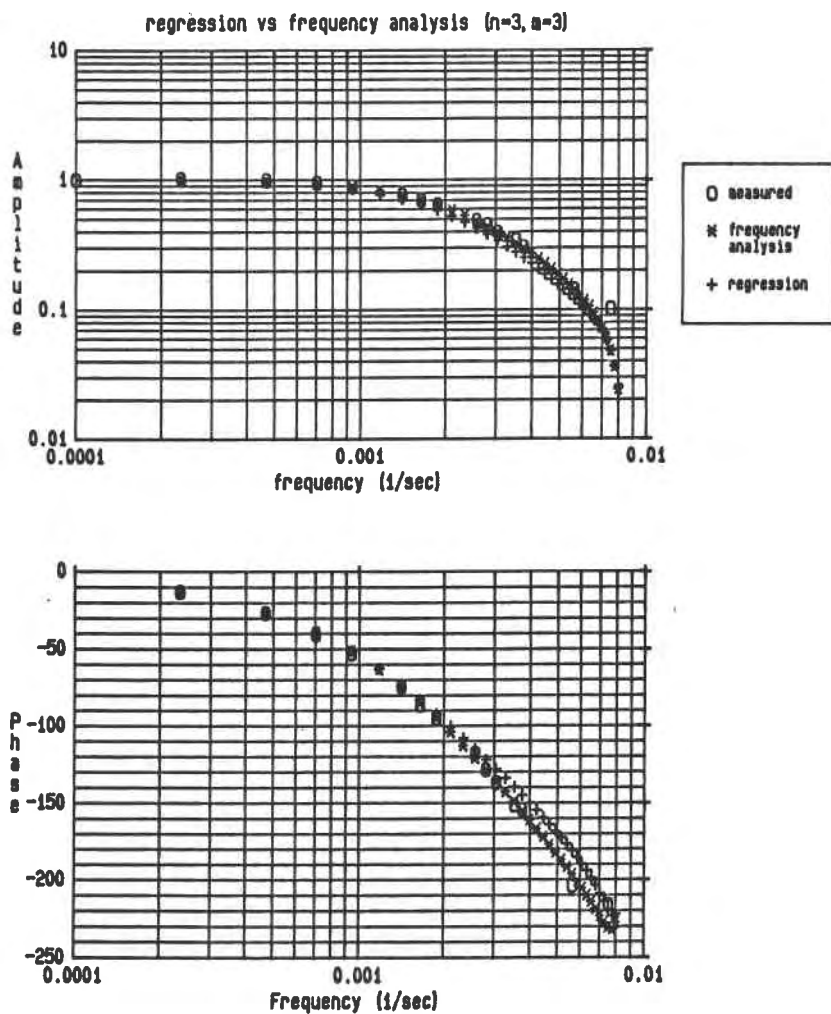


FIGURE 10. Frequency response of z -transfer functions; coefficients ($n = 3, m = 3$) obtained from frequency analysis and from time series regression. (See Tables 1 and 2.)

Table 2. *Z-transfer function coefficients from regression analysis ($\Delta = 60$ sec).*

| n | m | a_0 | a_1 | a_2 | a_3 | b_1 | b_2 | b_3 |
|---|---|-------|-------|-------|-------|-------|-------|-------|
| 3 | 3 | 0.023 | 0.232 | 0.243 | 0.044 | -.233 | -.328 | 0.102 |

Multiple linear regression was also applied directly to the time domain data by fitting coefficients to Equation (4). The resulting coefficients are given in Table 2, and the frequency response shown in Figure 10.

The results were better than expected, since both the authors had experienced difficulty with direct fitting of *ZTF* coefficients to data obtained using pulse or step signals as input. This is probably due to the much better frequency distribution of the BMFS excitation. To examine the susceptibility of the analysis to noisy data the input and output were corrupted by rounding to the nearest degree K and nearest 15 watts/m² respectively. Both time domain and frequency domain analysis on this "imprecise" data were stable. The results are given in Appendix C.

SUMMARY AND CONCLUSIONS

In general, the determination of dynamic response involves the following steps: select the form of the model; devise a test apparatus capable of maintaining the boundary conditions and measuring input and output variables; excite with an input signal; fit the model parameters to the measured data.

The application of system identification techniques was demonstrated by the experimental determination of dynamic thermal response characteristics of a small homogenous sample. The form of the model was predetermined to be the *z*-transfer function expressed as a ratio of polynomials [Equation (3)]. An experiment was devised to maintain the boundary condition of constant Θ_2 while values of Q_2 and Θ_1 were measured.

A binary multi-frequency sequence (BMFS) was chosen as the input excitation for Θ_1 . This type of signal has several attractive characteristics for system identification. It is easy to produce, requiring no complex waveform generator or precise control. It minimizes the disturbance to the system under test; the mean temperature for the sample tested varied by less than 5°C. It is efficient at concentrating power at appropriate frequencies; a step input has its energy concentrated at low frequencies, while a pulse contains the entire spectrum but at very low amplitudes. The BMFS, in combination with Fourier analysis, takes much less time than testing with an equivalent number of sinusoidal inputs.

Two methods were used to fit *ZTF* coefficients to the data. conventional multi-linear regression in time domain gave good results, despite the fact

Table 3. Frequency response of Z-transfer functions compared to measured response.

| Frequency (hz) | Amplitude | | | | | Phase | | | | |
|-------------------|-----------|-----------------|-----------------|-----------------|-----------------|----------|-----------------|-----------------|-----------------|-----------------|
| | Measured | n = 3, m = 4 | n = 3, m = 3 | n = 2, m = 2 | n = 2, m = 1 | Measured | n = 3, m = 4 | n = 3, m = 3 | n = 2, m = 2 | n = 2, m = 1 |
| 0.0 | 1.000 | 1.004 | 1.004 | 1.004 | 1.004 | 0.0 | 0.0 | 0.0 | 0.0 | 0.0 |
| 0.000235 | 1.020 | 0.995 | 0.996 | 0.995 | 0.992 | -13.0 | -13.3 | -13.2 | -13.3 | -14.0 |
| 0.000470 | 0.998 | 0.967 | 0.972 | 0.969 | 0.957 | -26.9 | -26.4 | -26.2 | -26.3 | -27.7 |
| 0.000704 | 0.957 | 0.927 | 0.934 | 0.929 | 0.905 | -40.5 | -39.0 | -38.9 | -39.0 | -40.7 |
| 0.000939 | 0.895 | 0.876 | 0.885 | 0.878 | 0.844 | -53.0 | -51.1 | -51.2 | -51.1 | -52.8 |
| 0.001408 | 0.770 | 0.763 | 0.769 | 0.761 | 0.718 | -74.2 | -73.5 | -74.1 | -73.6 | -74.4 |
| 0.001643 | 0.697 | 0.705 | 0.707 | 0.700 | 0.658 | -86.4 | -83.9 | -84.7 | -83.9 | -84.0 |
| 0.001878 | 0.651 | 0.648 | 0.647 | 0.642 | 0.604 | -95.7 | -93.9 | -94.6 | -93.6 | -93.0 |
| 0.002582 | 0.487 | 0.491 | 0.466 | 0.488 | 0.467 | -118.1 | -120.7 | -120.9 | -119.6 | -117.2 |
| 0.002816 | 0.455 | 0.444 | 0.441 | 0.444 | 0.430 | -128.4 | -128.7 | -128.6 | -127.3 | -124.6 |
| 0.003051 | 0.396 | 0.402 | 0.400 | 0.404 | 0.396 | -136.8 | -136.1 | -135.8 | -134.6 | -131.7 |
| 0.003521 | 0.345 | 0.327 | 0.329 | 0.334 | 0.336 | -151.5 | -149.5 | -149.1 | -148.2 | -145.3 |
| 0.003756 | 0.305 | 0.296 | 0.299 | 0.304 | 0.310 | -154.4 | -155.5 | -155.2 | -154.6 | -151.8 |
| 0.005634 | 0.144 | 0.144 | 0.143 | 0.138 | 0.154 | -204.0 | -193.0 | -196.2 | -195.8 | -200.0 |
| 0.007512 | 0.102 | 0.058 | 0.049 | 0.048 | 0.044 | -216.3 | -236.5 | -230.4 | -209.9 | -239.7 |

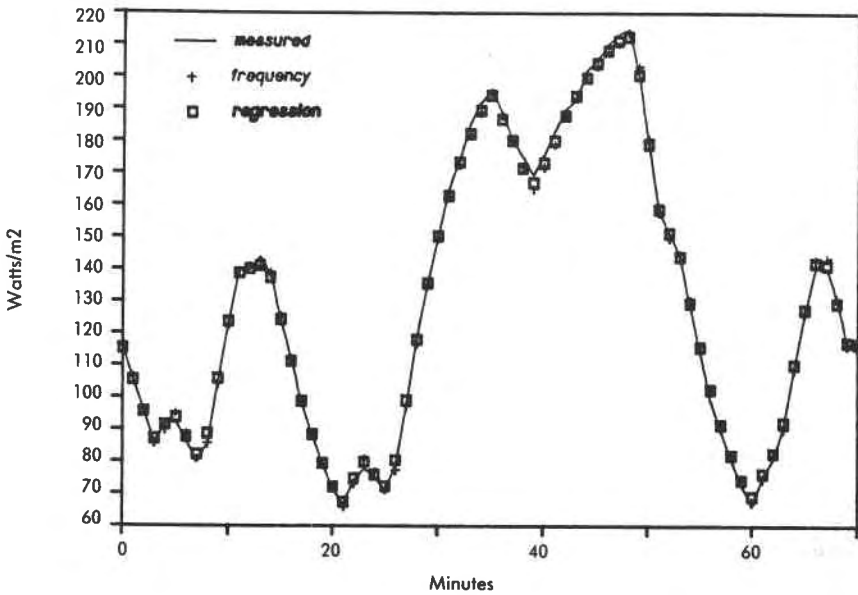


FIGURE 11.

that previous experience with other forms of input signal had shown problems. This might be attributed to the much better frequency distribution characteristics of the BMFS.

An alternative method of fitting *ZTF* coefficients is to first obtain the response of the system at a number of frequencies using Fourier analysis, and then use linear regression to fit coefficients to the frequency response data. This technique gives a much better picture of how the system responds at different frequencies. Anomalies in the test results are much more apparent when examining frequency response since the general form of the Bode plot is known. This technique should be less susceptible to noise, and also permits the sampling interval for the *z*-transform to be different from that of the data in the test.

Each of these methods can give a number of different sets of coefficients, which are a good representation of the dynamic response; they tend to differ only at the higher frequencies.

The experiment indicated that regression in both time domain and frequency domain was robust when applied to data from the BMFS excitation. This was tested by decreasing the resolution of input and output signals to 1°C and 15 watt/m^2 respectively. Analysis of this "imprecise" data yielded the transfer functions shown in Appendix C.

The laboratory demonstration on a small homogenous sample indicates that testing using BMFS and frequency analysis has promise for determining dynamic thermal response. This technique is currently being extended, at Concordia University, to larger scale testing on samples of more typical wall construction. By devising a test apparatus with appropriate boundary conditions one could apply it to determination of the other functions in the transmission matrix of Equation (1). Since this type of testing has long been used in process industries it could be well suited to determining the dynamic characteristics of other elements, such as HVAC system components, providing these satisfy the restriction that the systems can be considered linear.

ACKNOWLEDGEMENTS

The work described in this paper was carried out at the Institute for Research in Construction at National Research Council Canada with financial support from the Natural Sciences and Engineering Research Council. The authors are grateful for the advice and assistance of their colleagues at IRC/NRCC, and especially to R. G. Marchand of the Thermal Insulation Laboratory for making the measurements.

APPENDIX A

Description of Sample

The test sample is a rubber material. The following properties were determined by laboratory measurement:

| | |
|------------------------------------|----------------------------|
| Density (ρ) | = 1252.1 kg/m ³ |
| Specific heat (C_p) | = 1073.5 J/kgK |
| Thermal conductivity (λ) | = 0.2314 W/mK |
| Thickness (ℓ) | = 0.0123 m |

The transfer function Q_2/Θ_1 , in Laplace transform notation, is (from Reference 4)

$$H_{(s)} = \frac{\lambda\sqrt{s/\alpha}}{\sinh(\ell\sqrt{s/\alpha})} \quad (\text{A1})$$

where $\alpha = \lambda/(C_p\rho)$ is the thermal diffusivity.

The theoretical frequency response is obtained by substituting $j\omega$ for s :

$$H_{(\omega)} = \frac{\lambda\sqrt{j\omega/\alpha}}{\sinh(\ell\sqrt{j\omega/\alpha})} \quad (\text{A2})$$

APPENDIX B

Derivation of Z-Transfer Function Coefficients from Frequency Response Data

The form of the z -transfer function is

$$H_{(z)} = \frac{a_0 z^0 + a_1 z^{-1} + a_2 z^{-2} + \dots + a_n z^{-n}}{1 + b_1 z^{-1} + b_2 z^{-2} + \dots + b_m z^{-m}} \quad (\text{B1})$$

where

$a_0 \dots a_n, b_1 \dots b_m$ = coefficients

z^{-i} = operator representing a time delay = $i\Delta$ where Δ is the time interval for calculation.

Since $z = e^{\Delta s}$, Equation (B1) in Laplace notation becomes

$$H_{(s)} = \frac{a_0 + a_1 e^{-\Delta s} + a_2 e^{-2\Delta s} + \dots + a_n e^{-n\Delta s}}{1 + b_1 e^{-\Delta s} + b_2 e^{-2\Delta s} + \dots + b_m e^{-m\Delta s}} \quad (\text{B2})$$

Substituting $j\omega$ for s ,

$$H_{(\omega)} = \frac{a_0 + a_1 e^{-j\omega\Delta} + a_2 e^{-2j\omega\Delta} + \dots + a_n e^{-nj\omega\Delta}}{1 + b_1 e^{-j\omega\Delta} + b_2 e^{-2j\omega\Delta} + \dots + b_m e^{-mj\omega\Delta}} \quad (\text{B3})$$

or, since $e^{-j\omega\Delta} = \cos \omega\Delta - j \sin \omega\Delta$,

$$H_{(\omega)} = \frac{a_0 + a_1 [\cos(\omega\Delta) - j \sin(\omega\Delta)] + a_2 [\cos(2\omega\Delta) - j \sin(2\omega\Delta)] + \dots}{1 + b_1 [\cos(\omega\Delta) - j \sin(\omega\Delta)] + b_2 [\cos(2\omega\Delta) - j \sin(2\omega\Delta)] + \dots} \quad (\text{B4})$$

$$\frac{\dots + a_n [\cos(n\omega\Delta) - j \sin(n\omega\Delta)]}{\dots + b_m [\cos(m\omega\Delta) - j \sin(m\omega\Delta)]}$$

H is a complex value consisting of a real part H_R and an imaginary part H_I . Equating the real and imaginary parts of Equation (B4) yields

$$H_{R(\omega)} = a_0 + a_1 \cos(\omega\Delta) + a_2 \cos(2\omega\Delta) + \dots + a_n \cos(n\omega\Delta) - b_1 [H_{R(\omega)} \cos(\omega\Delta) + H_{I(\omega)} \sin(\omega\Delta)] - \dots \quad (\text{B5})$$

$$- b_m [H_{R(\omega)} \cos(m\omega\Delta) + H_{I(\omega)} \sin(m\omega\Delta)]$$

$$H_{I(\omega)} = -a_1 \sin(\omega\Delta) - a_2 \sin(2\omega\Delta) - \dots - a_n \sin(n\omega\Delta) + b_1 [H_{R(\omega)} \sin(\omega\Delta) - H_{I(\omega)} \cos(\omega\Delta)] + \dots \quad (\text{B6})$$

$$+ b_m [H_{R(\omega)} \sin(m\omega\Delta) - H_{I(\omega)} \cos(m\omega\Delta)]$$

Table C1. Z-transfer function coefficients from frequency analysis ($\Delta = 60$ sec).

| n | m | a_0 | a_1 | a_2 | a_3 | a_4 | b_1 | b_2 | b_3 | b_4 |
|---|---|-------|-------|-------|-------|-------|--------|-------|-------|-------|
| 2 | 1 | 0.0 | 0.210 | 0.210 | — | — | -.580 | — | — | — |
| 2 | 2 | 0.0 | 0.213 | 0.190 | — | — | -.659 | 0.062 | — | — |
| 3 | 3 | 0.0 | 0.201 | 0.074 | -.140 | — | -1.277 | 0.426 | -.015 | — |
| 3 | 4 | 0.0 | 0.208 | 0.080 | -.098 | — | -1.246 | 0.568 | -.227 | 0.095 |

The Equations (B5) and (B6) can be written for each frequency for which response data is available. In addition, for the steady state condition ($\omega = 0$) Equation (B3) reduces to

$$U = \frac{a_0 + a_1 + \dots + a_n}{1 + b_1 + b_2 + \dots + b_m} \quad (\text{B7})$$

where U is the steady state U -value.

Thus, if response data for N frequencies is available then $2N + 1$ equations result; these can easily be solved for the coefficients (a_0 to a_n and b_0 to b_m) using multiple linear regression provided the number of coefficients ($n + m + 1$) is less than the number of equations. Equation (B7) can be given extra weight to ensure that the z -transfer function has the correct steady state U -value.

A complication may arise when phase lags of 180° occur. Under this condition the regression may produce negative values for a_0 . This can be prevented by forcing a_0 to zero in Equations (B5) and (B7).

APPENDIX C

Analysis Using Imprecise Data

Experience has shown that regression techniques often work well with very precise data, but fail when noise is present in the data. To examine the robustness of the techniques employed in this paper the data was made less precise by rounding the input (temperature difference) to the nearest degree Kelvin and the output (heat flow) to the nearest watt, which corresponds to approximately 15 w/m^2 . This represents approximately a hundredfold reduction in measured precision.

Frequency response analysis was then carried out on this "corrupted" data. The response obtained is shown in Figure C1. While there is obviously some loss of information due to the reduced precision the frequency response obtained does not differ

Table C2. Z-transfer function coefficients from regression analysis ($\Delta = 60$ sec).

| n | m | a_0 | a_1 | a_2 | a_3 | b_1 | b_2 | b_3 |
|---|---|-------|-------|-------|-------|-------|-------|-------|
| 3 | 3 | 0.031 | 0.238 | 0.169 | 0.065 | -.456 | -.053 | 0.012 |

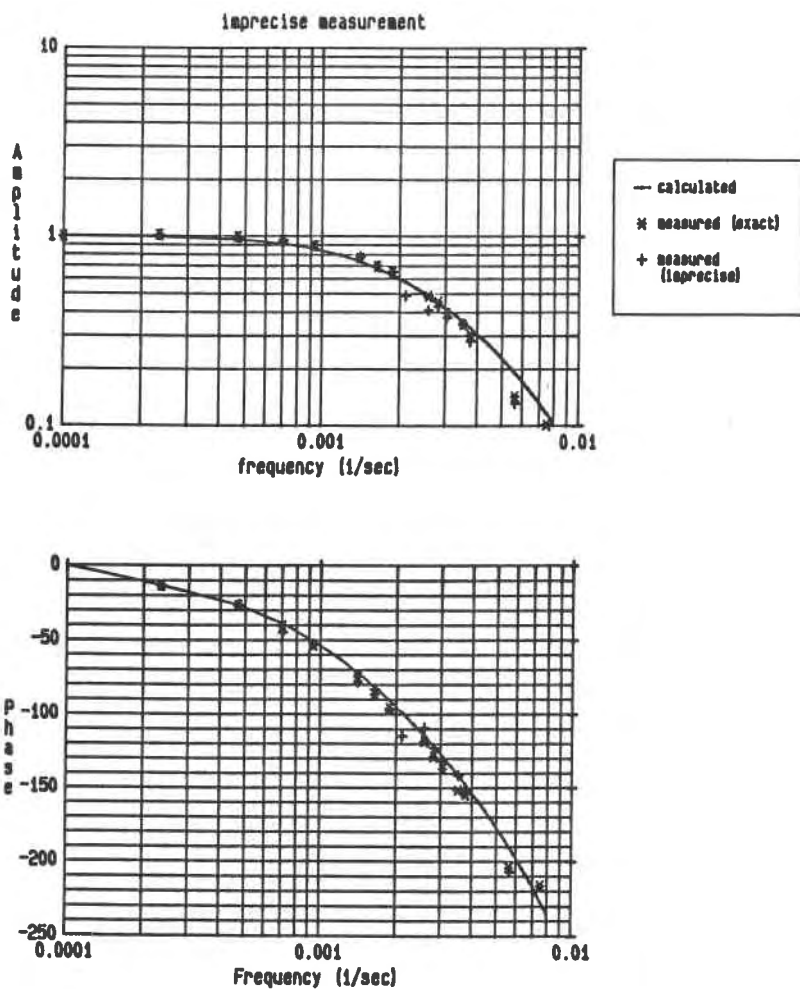


FIGURE C1. Frequency response obtained from test data made imprecise through rounding to nearest degree and nearest 15 w/m² (approximately 100 times less precision than actual measurement).

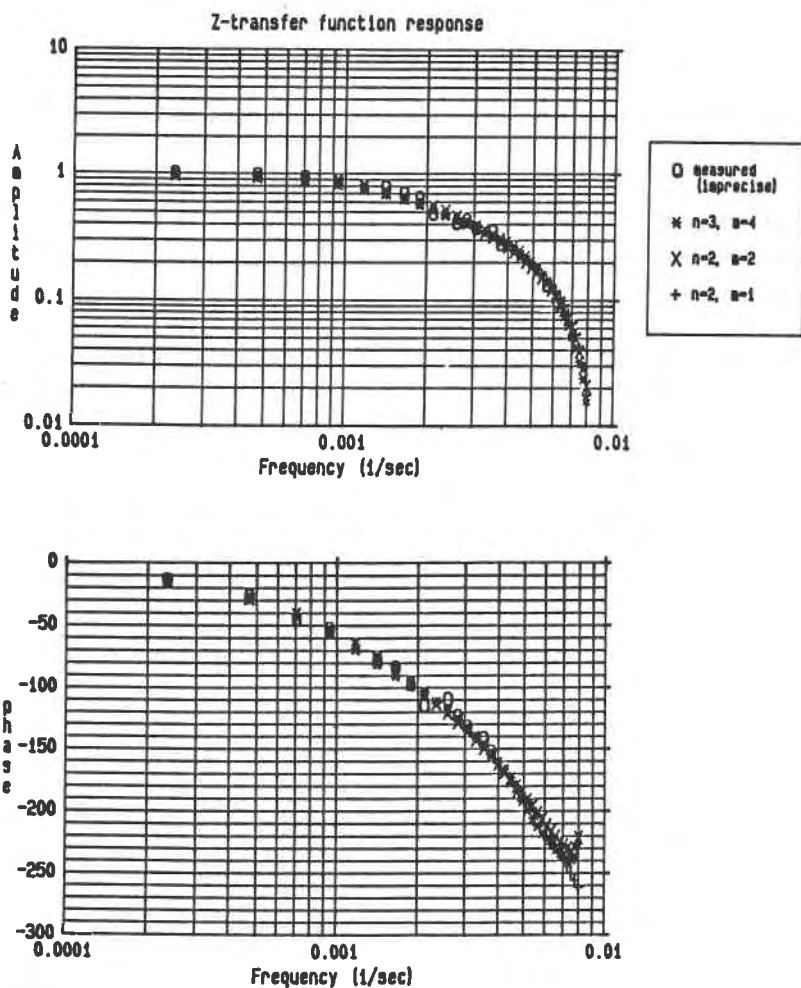


FIGURE C2. Frequency response of z -transfer functions obtained by fitting to frequency analysis of imprecise data. Coefficients are given in Table C1.

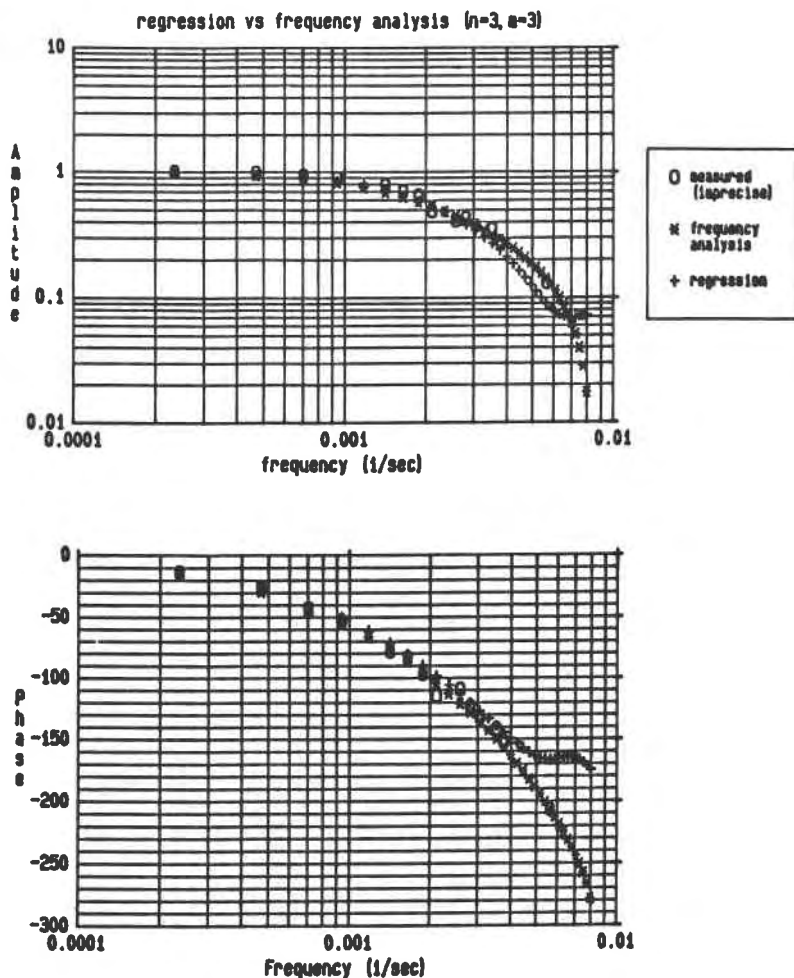


FIGURE C3. Frequency response of z -transfer functions ($n = 3, m = 3$) obtained from frequency analysis and from time series regression of imprecise data. (See Tables C1 and C2 for coefficients.)

greatly from that obtained from the precise measurement. Z -transfer function coefficients obtained by fitting to this frequency response are given in Table C1. All of these produced stable simulations. Figure C2 shows the frequency response of the z -transfer functions.

Regression analysis was also carried out on the imprecise data. The resulting z -transfer function coefficients, given in Table C2, give a stable simulation. However, as shown in Figure C3, the frequency response of the z -transfer function from regression is somewhat distorted at high frequencies.

REFERENCES

1. ASHRAE Handbook of Fundamentals.
2. Stephenson, D. G. and G. P. Mitalas. "Calculation of Heat Conduction Transfer Function for Multi-Layer Slabs," *ASHRAE Transactions*, V. 77, Part II (1971).
3. Mitalas, G. P. and J. G. Arseneault. "Fortran IV Program to Calculate Z-Transfer Functions for the Calculation of Transient Heat Transfer Through Walls and Roofs," National Research Council Canada, Division of Building Research, CP 33 (1972).
4. Pipes, L. A. "Matrix Analysis of Heat Transfer Problems," *Franklin Institute Journal*, 263(3):195-205 (1957).
5. Astrom, K. J. and P. Eykhoff. "System Identification—A Survey," *Automatica*, 7(2):123-162 (1971).
6. Bekey, G. A. "System Identification—An Introduction and a Survey," *Simulation*, 15(4):151-166 (1970).
7. Sinha, N. K. and B. Kuszta. *Modelling and Identification of Dynamic Systems*. Van Nostrand Reinhold Company (1983).
8. Nagrath, I. J. and M. Gopal. *Control Systems Engineering*. 2nd edition. Halsted Press (1982).
9. Mitalas, G. P. "Calculation of Transient Heat Flow Through Walls and Roofs," *ASHRAE Transactions*, V. 74, Part II (1968).
10. Van den Bos, A. "Construction of Binary Multi-Frequency Signals," IFAC Symp. (1967).
11. Grawford, R. R. and J. E. Woods. "A Method for Deriving a Dynamic System Model from Actual Building Performance Data," *ASHRAE Transactions*, V. 91, Part 2 (1985).
12. Pedersen, C. O. and E. D. Mouen. "Application of System Identification Techniques to the Determination of Thermal Response Factors from Experimental Data," *ASHRAE Transactions*, V. 79, Part 2, pp. 127-136 (1973).
13. Sherman, M. H., R. E. Sonderegger and J. W. Adams. "The Determination of the Dynamic Performance of Walls," *ASHRAE Transactions*, V. 88, Part 1 (1982).
14. Bomberg, M. and K. R. Solvason. "Comments on Calibration and Design of a Heat Flow Meter," Thermal Insulation, Materials, and Systems for Energy Conservation in the '80s, ASTM STP 789, American Society for Testing and Materials, pp. 277-292 (1983).
15. Bergland, G. S. "A Guided Tour of the Fast Fourier Transform," *IEEE Spectrum*, pp. 41-52 (July, 1969).
16. IMSL Stat/PC Library (1984).

This paper is being distributed in reprint form by the Institute for Research in Construction. A list of building practice and research publications available from the Institute may be obtained by writing to the Publications Section, Institute for Research in Construction, National Research Council of Canada, Ottawa, Ontario, K1A 0R6.

Ce document est distribué sous forme de tiré-à-part par l'Institut de recherche en construction. On peut obtenir une liste des publications de l'Institut portant sur les techniques ou les recherches en matière de bâtiment en écrivant à la Section des publications, Institut de recherche en construction, Conseil national de recherches du Canada, Ottawa (Ontario), K1A 0R6.